Journal of South American Earth Sciences 106 (2021) 102903

Contents lists available at ScienceDirect

Journal of South American Earth Sciences

journal homepage: www.elsevier.com/locate/jsames

The architecture of the Eopaleozoic Cococi Basin, northeastern Brazil: 2D geological modelling from magnetic and gravimetric data

Francisco Fernando B. dos S. Filho [a,b,*], Christiano Magini [a], Sebastián González Chiozza [a], Raimundo Mariano G. Castelo Branco [a,b]

[a] Department of Geology, Federal University of Ceará, Fortaleza, Ce, Brazil
[b] Laboratory of Geophysics Prospecting and Remote Sensing, No. 1011, Department of Geology, Federal University of Ceará, Fortaleza, Ce, Brazil

ARTICLE INFO

Keywords:
Minimum curvature
Analytic signal
Euler deconvolution
2D modeling

ABSTRACT

Cococi Basin is a small Eopaleozoic syneclise that is overlying basement rocks of the Neoproterozoic Central Ceará Domain of the Borborema Province, northeastern Brazil. Its origin is associated with the final stages of the Brasiliano orogenic cycle (600 My). The Basin classified as rift type has its basement constituted by rocks of the Canindé Unit and the crosshead complex and delimited by Senador Pompeu and Tauá shear zones. Three geophysical cross-sections were created using aero-magnetometric and field gravimetric data, aiming to outline the litho-structural underground features of the Basin. We have used the following methods for processing and interpreting geophysical data: *minimum curvature*, *analytic signal amplitude, Euler deconvolution,* and *2D modeling*. The obtained depth solutions were interpreted and combined with geological data to generate geological models featuring the limits and depth of the Basin, its internal main structures, and its lithological variations. The developed geophysical-based geological modeling unravels the yet unknown geological features of the Cococi Basin, which corroborates with geological field observations, surface mapping and the results of previous investigations.

1. Introduction

The (CB) was formed by an Eopaleozoic syneclise located between the Central Ceará and Rio Grande do Norte Domains, within the Borborema Province, northeast Brazil (Fig. 1). According to Parente et al. (2004), this regional structure classifies as a rift type Basin, which has its origin associated with re-activation movements of the Tauá shear zone and Senador Pompeu shear zone, in a system that progressively evolved from a compressive to a (extensional) tectonic regime.

At the western part of the Borborema Province, several other Basins such as Jaibaras (Pedrosa et al., 2015), Catolé (Parente and Arthaud, 1995), Carnaubinha and São Bento and Iara (Parente et al., 2004) were originated by similar processes. Most of these Basins and their basements nearby host important copper occurrences that have been the objective of the study of exploration companies since the 1970′s. Defining the major structures associated with these Basins and their basement is essential to identify possible fluid conducts and regions which are more prone to host copper mineralization.

A variety of geophysical methods are frequently used to map the interior of the Earth and infer the structure of the lithosphere. Potential methods, such as gravimetry and magnetometry, are suitable for studying paleo-continental rift settings, where the main structural features occur at the subsurface within the upper 10 km of the Earth's crust. In such context, gravity and magnetic data could be successfully applied to infer the horst-graben geometry of the Basins, estimate fracture density variations, as well as to detect magmatic rocks and ore occurrences (Soares, 2011), (Castro et al., 2012), (Pedrosa et al., 2015) and (Oliveira et al., 2018).

In this paper, we present a tectonic analysis of the CB based on bi-dimensional gravimetric models and aeromagnetic data.

2. Geological setting

The Cococi Basin originated during the ultimate stage of the Brasiliano/Pan-African orogeny that led to West Gondwana amalgamation between 660 and 570 My. At the end of the orogeny, the collisional

* Corresponding author. Department of Geology, Federal University of Ceará, Fortaleza, Ce, Brazil.
E-mail addresses: franciscofernandob@gmail.com (F.F.B.S. Filho), magini2005@hotmail.com (C. Magini), gercharrems@yahoo.com (S.G. Chiozza), marianogcb@gmail.com (R.M.G. Castelo Branco).

https://doi.org/10.1016/j.jsames.2020.102903
Received 25 March 2020; Received in revised form 11 September 2020; Accepted 14 September 2020
Available online 6 October 2020

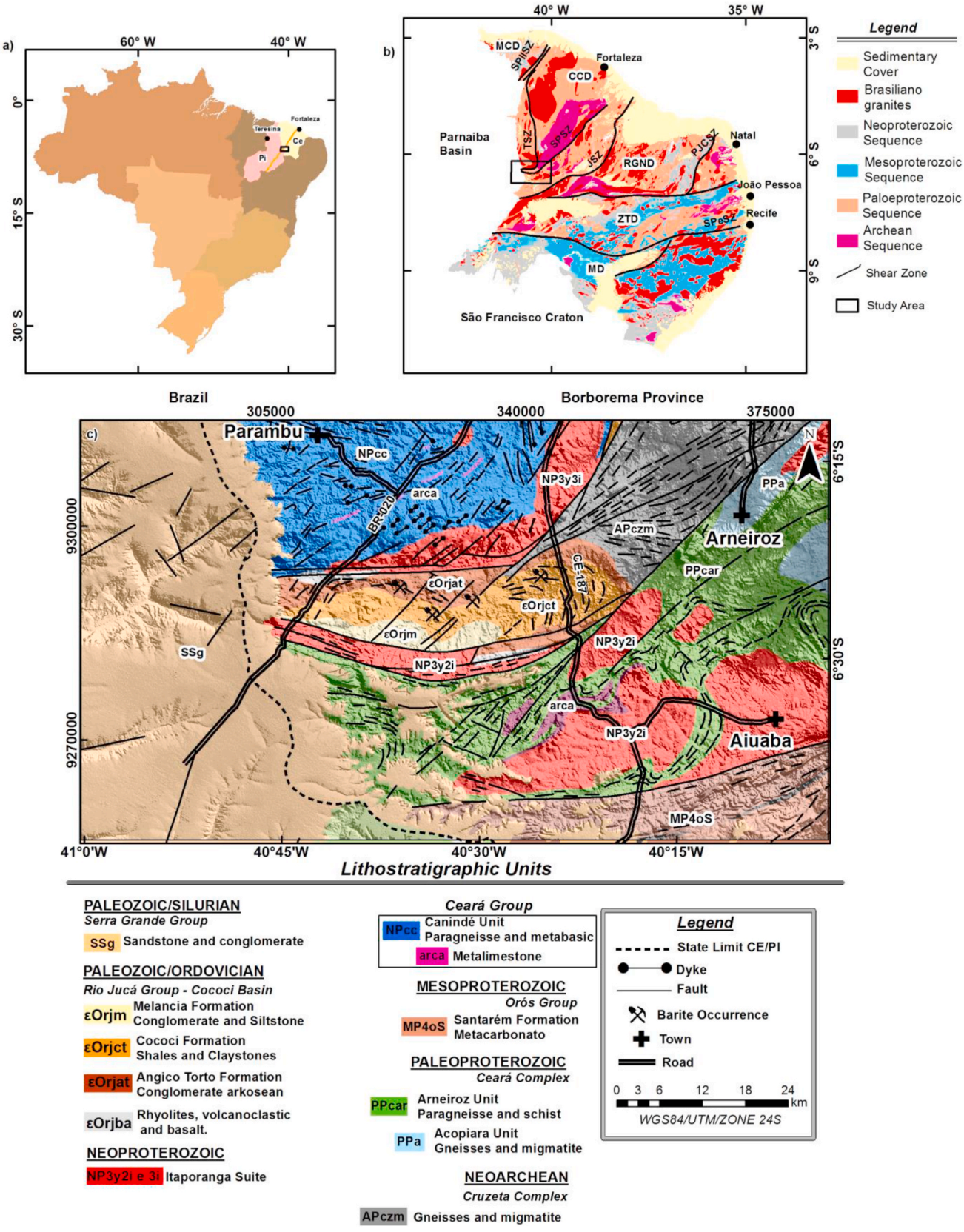

Fig. 1. a) Location of the Cococi Basin in the NE Brazil; b) Simplified map of the Borborema province adapted from Pedrosa Jr et al. (2015) with its tectonic domains (DMC: Médio Coreau – DCC: Ceará Central – DRGN: Rio Grande do Norte – DZT: Zona Transversal – DM: Meridional) and main shear zones (SPSZ II: Sobral-Pedro II – TSZ: Tauá – SPSZ: Senador Pompeu – JSZ: Jaguaribe – PJCSZ: Pucuí-João Câmara – PeSZ: Pernambuco); c) Simplified geologic map of Cococi Basin (Cavalcante et al., 2003).

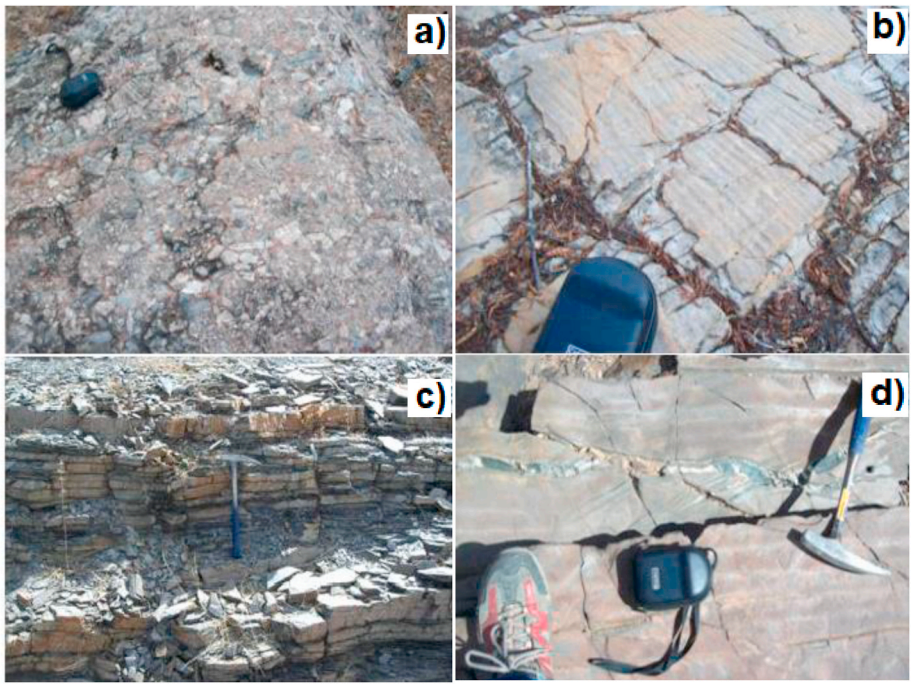

Fig. 2. (a) Polimitic conglomerate. (b) ripple marks on sandstone (c) Rhythmic shales. (d) Limestone showing fracture with basalt injection and calcite veins.

process twisted from frontal to oblique, generating regional scale dextral shear zones (Arthaud, 2007). Later, the region became dominated by a post-collisional extensional stress regime, which led to the development of several rift Basins through the reactivation of the late-collisional shear zones. Situated at the western portion of the Borborema Province, the Cococi rift is bounded at north and south by the E-W trending shear zones. Its western portion is partially covered by the Silurian sedimentary rocks of the Serra Grande Group (Parnaiba Basin).

Including its covered part, the Basin extends for about 67 km in E-W direction and is approximately 20 km wide. The Cococi Basin is mainly composed of molasse sedimentary rocks, which discordantly overlie the Pre-Cambrian basement and are affected by half-graben structures (Gomes et al., 2000).

The Basin's stratigraphy is divided into two distinguished periods (Vasconcelos and Gomes, 1998): 1) The Ediacaran – Cambrian period, represented by Angico Torto and Cococi Formations; 2) The Cambrian – Ordovician period, represented by the Melancia Formation and the synchronous bimodal vulcanism. The basal Angico Torto Formation outcrops at the northern border of the Basin and is composed of arkosean conglomerates (Fig. 2a) with fine-grained sandstones showing ripple marks (Fig. 2b) with siltstones intercalations towards the top. The Cococi Formation overlies the Angico Torto Formation and is dominated by shales, claystones and calcareous siltstones; The top sedimentary sequence is represented by the Melancia Formation, which is mainly composed of conglomerates and sedimentary breccias, with local intercalations of fine-grained sandstones, siltstones and rhythmites within the upper portion (Fig. 2c). According to Gomes et al. (2000), the three formations within the Cococi Basin correspond to an alluvial fan environment. However, besides the sedimentary rocks described as the formations, synchronous vulcanic associations occurred with the evolution of the Basin. The latter consists of rhyolites and green polymitic volcaniclastics rocks mitic in the northern limit of the Basin, bodies of basalts in the form of dikes, and extensive sills also occur in the southern border. In addition, it was observed basalt dikes injected in the limestone Fig. 2d) were also found, showing synchronism between sedimentation and vulcanism.

The Cococi rift divides the alkali granitic association of the Neoproterozoic Itaporanga suite into the two parts, which appear bordering the Basin at the south and the north. The underlying and surrounding Precambrian basement is partially composed by igneous derived gneisses and migmatites of the Archean Cruzeta Complex (2.7 Gy) outcropping to the west (Fetter et al., 2000; Martins et al., 2009), and by the metapelitic sequences encompassed by the Neoproterozoic Ceará Group (750-650 My) (Arthaud, 2007).

3. Geophysical data

3.1. Aeromagnetic data

The aeromagnetic data were supplied by the Brazilian Geological Survey (CPRM), which carried out the acquisition during the Borda Leste da Bacia do Maranhão aerogeophysical project in 1979 (Fig. 4). Flight lines were executed in N30°W direction and at 500 m height with a 2 km spacing; whereas control lines were oriented N60°E and spaced 20 km. Aeromagnetic data were processed according to the following routine: i) data interpolation in a 500 m spaced regular grid through the Bigrid method (Billings and Richards, 2000); ii) micro-leveling with directional cosine filter to eliminate the high-frequency background noise produced by the aircraft during acquisition; iii) filtering residual and regional responses to enhance the magnetic anomalies of superficial sources within the upper crust; iv) centering anomalies with their respective sources; v) 1st order vertical derivative and tilt both used to enhance shallow sources, mainly linear structural, and vi) analytical signal amplitude, which objective is to improve the sources of high frequency, helping with the interpretation of magnetic domains.

3.2. Gravimetric data

Field gravimetric data acquisition was carried out along main and secondary roads, following an N-S trend, perpendicular to the main geological structures. A total of 190 measuring stations were distributed in three sections, S1, S2, and S3, with an approximate extension of 30 km each. Spacing between stations was to 0.5 km within the sedimentary Cococi Basin to assure a good resolution within the Basin, and 1 km for the granitic rocks of the intrusive suite, and 2 km for the parametamorphic rocks. The Bouguer anomaly computed and calculated

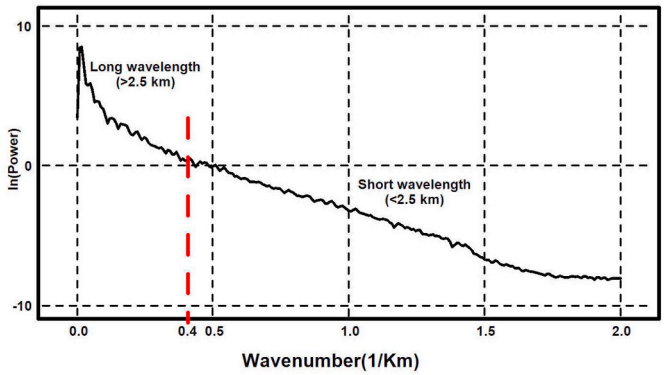

Fig. 3. Radially averaged power spectrum of magnetic data of the study area with the estimate cutoff wavelength 2.5 km.

using standard corrections for latitude, elevation, topography, instrumental drift and tidal influence were performed. The best-fitting regional surfaces for the observed anomaly data were determined by least squares (1st order polynomial), and then, used for calculating the residual anomaly. The resulting residual component of the gravimetric field is defined between −6 and 3.5 mGal.

It was applied semi-automatic source-detection methods to assist the analysis and interpretations of the geophysical data to be processed. Therefore, *curvature* was applied to magnetic data, *analytic signal* and *Euler deconvolution* were applied to both magnetic and gravimetric data, and *2D modeling* was done exclusively using gravimetric data.

4. Data processing methods

4.1. Curvature

Phillips et al. (2007) showed that potential field anomalies could be transformed in special functions that exhibit peaks or a variety of ridges that are isolated from the sources and their values are related to the depth of such sources. The direction and depth of the source is computed through the auto values and auto vectors of a regular grid, which is obtained with a quadratic matrix. In this work, it was used the auto values and auto vectors estimation method through the horizontal gradient magnitude (Hgm, Cordell and Grauch, 1985) to identify linear structures from magnetic data. In addition to determining the location and amplitude of the anomaly crest, the quadratic-surface approach provides the strike of the source and the 'most negative' curvature of the quadratic surface, which is used to estimate the source depth.

4.2. Regional and residual anomalies

The power spectrum of the magnetic signal was generated in order to separate spectrally shallow and deep sources causative of the magnetic anomaly. The regional and residual components of the magnetic field were separated by a regional-residual separation filter based on the Gaussian distribution of magnetic sources according to the wavenumber. The filter is a mathematical operator that acts as a low-pass or high-pass of frequencies within a selected band based on the wavelength represented in the power spectrum as wavenumber (Fig. 3). The Gaussian function standard deviation of 0.4 rad/km representing a cutoff wavelength of approximately 2.5 km was used to separate the sources regional and residual anomalies.

4.3. Analytic signal

According to Blakely (1996), the analytic signal amplitude is formed through the combination of the vertical and horizontal gradients of the anomalous magnetic field (AMF). This method depends on the position of the bodies but not on the direction of their magnetization (this parameter is only considered when performing magnetic anisotropy studies) and has been used by Nabighian (1972, 1974) to estimate the depth and position of the sources in two-dimensional bodies. Regarding the plausible behavior of the solution clouds, the investigation window size has been set in 1200 m.

According to Blakely (1996) the magnitude of the analytic signal is independent of the direction of magnetization for the two-dimensional case, and this can similarly be shown to be true for the

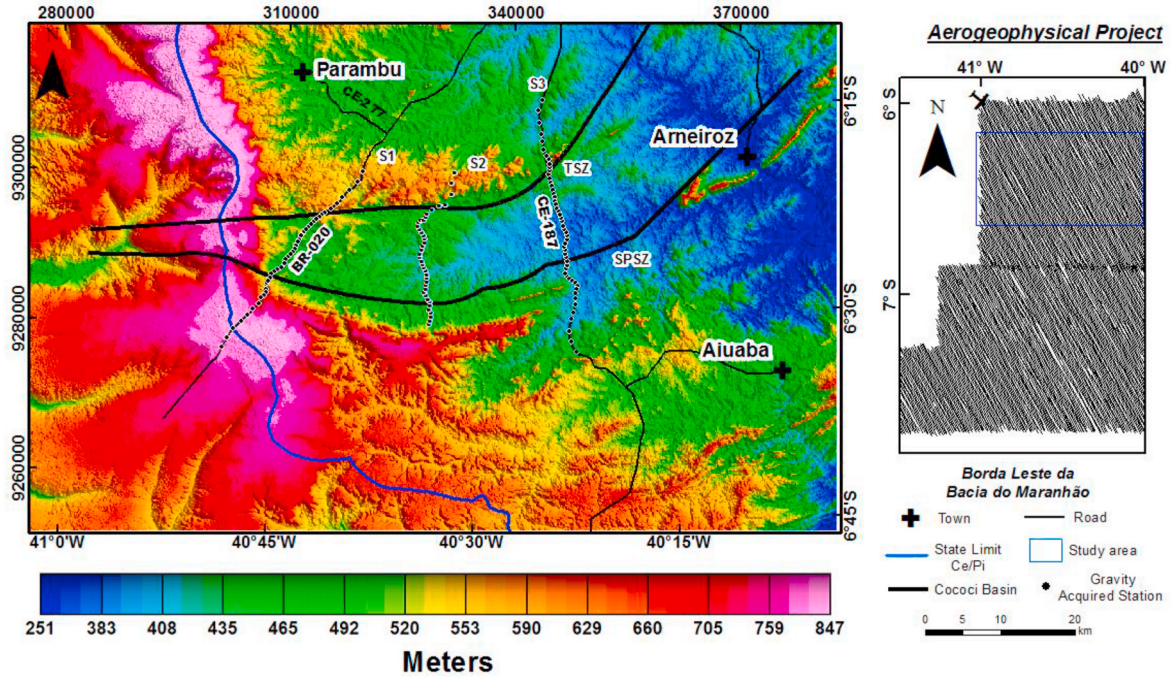

Fig. 4. Location map of the "Borda Leste da Bacia do Maranhão" aerogeophysical project (right) and the Digital Elevation Model (DEM) indicating the gravimetric profiles (S1, S2, S3) and stations (black points) (left). TSZ – Tauá shear zone and SPSZ – Senador Pompeu shear zone.

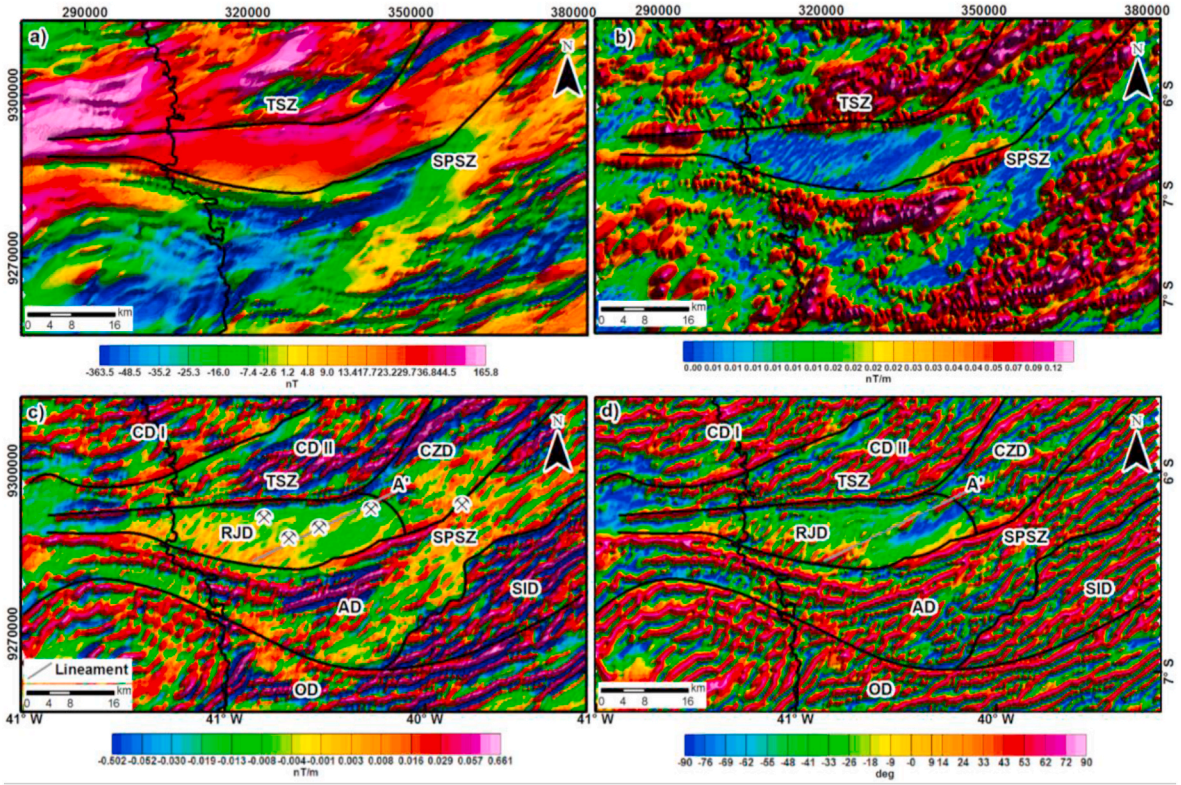

Fig. 5. a) Anomalous magnetic field map; b) Analytic signal amplitude map; c) first-order derivative map with identification of the magnetic domains; d) tilt derivative map and TSZ – Tauá shear zone and SPSZ – Senador Pompeu shear zone. CDI – Canindé Domain I; CDII – Canindé Domain II; CZD – Cruzeta Domain; AD – Arneiroz Domain; SID – Intrusive Suites Domain; OD – Orós Domain; RJD – Rio Jucá Domain.

three-dimensional case. Proposes Nabighian (1972), Roest et al. (1992), Macleod et al. (1993a, b) the use of 3-D analytic signal calculated from the total magnetic field as a practical alternative to reduction to the pole from low magnetic latitudes. In fact, this technique has merit at all magnetic latitudes, but the benefits are most apparent near the magnetic equator.

4.4. Tilt derivative

Many authors have suggested the use of directional and vertical derivatives to delimit causative sources in potential methods (Hood and Teskey, 1989; Roest et al., 1992) and Cordel and Grauch (1985) suggest using the full horizontal gradient. However, if the source is superimposed or several sources in its surroundings, the estimation through these methods will be compromised as well as the deep sources present low values and smaller gradients, it will not become noticeable, because it is the amplitude of the gradient that will be taken into consideration.

According to Miller and Singh (1994), the tilt angle overcomes this problem by dealing with the ratio of the vertical derivative to the horizontal gradient. Since both will be smaller for deeper sources, the ratio will still be large when over the source, pass through zero over, or near, the edge where the vertical derivative is zero and the horizontal gradient is a maximum, and will be negative outside the body where the vertical derivative is negative. By expressing this as a tilt angle rather than a ratio, it will always be in the range $-90° < \mathrm{TILT} < 90°$. The tilt angle will be relatively insensitive to the depth of the source and should resolve shallow and deep sources equally as well and to enable us to separate out the magnetic domains' directions (Fig. 5).

4.5. Euler deconvolution

The Euler deconvolution method is applied to both gravimetric and magnetometric data to obtain estimates of causative source location in depth (Doo et al., 2007). Although this technique is not based on a geological model, the elemental magnetic distributions should be interpreted regarding geological elements such as faults, plutons, dikes, or necks. These aspects, discussed by Hood and Teskey (1989), are expressed in equation (1):

$$(x - x_0)\frac{\partial f}{\partial x} + (y - y_0)\frac{\partial f}{\partial y} + z_0\frac{\partial f}{\partial z} = -N\Delta T(x, y) \quad (1)$$

where x_0, y_0, z_0 define the position of the magnetic source, represented by the anomalous magnetic field (T), x, y, z define the detection position and N is the magnetic force decay rate, which is related to the distance to the source and considered as the structural index. Based on Keating (1998), an N value of 0.5 has been adopted as it is adequate for estimating the source's geometry, highlighting contacts and comparing results with the local geological features. Regarding the plausible behavior of the solution clouds, the investigation window size has been set in 1250 m.

4.6. 2D modeling

In this work, it was used gravimetric modeling in GM-SYS (GM-SYS, 2004) software of the Oasis Montaj, based on the algorithm proposed by Won and Bevis (1987), which is based on the methods of Talwani et al. (1959) and Talwani and Heirtzler (1964). With this methodology, a geophysical model is created and its theoretical response (either magnetic or gravimetric) is calculated; therefore, the model is adjusted intuitively until the answer matches the surveying results. The gravity modeling consists of iterative methods or automated techniques, using data inversion procedures. The procedure estimates the depth of one or more interfaces that separate the geological medium according to density. The direct modeling compares and adjusts the calculated to the observed gravity values, determined by density contrasts and source

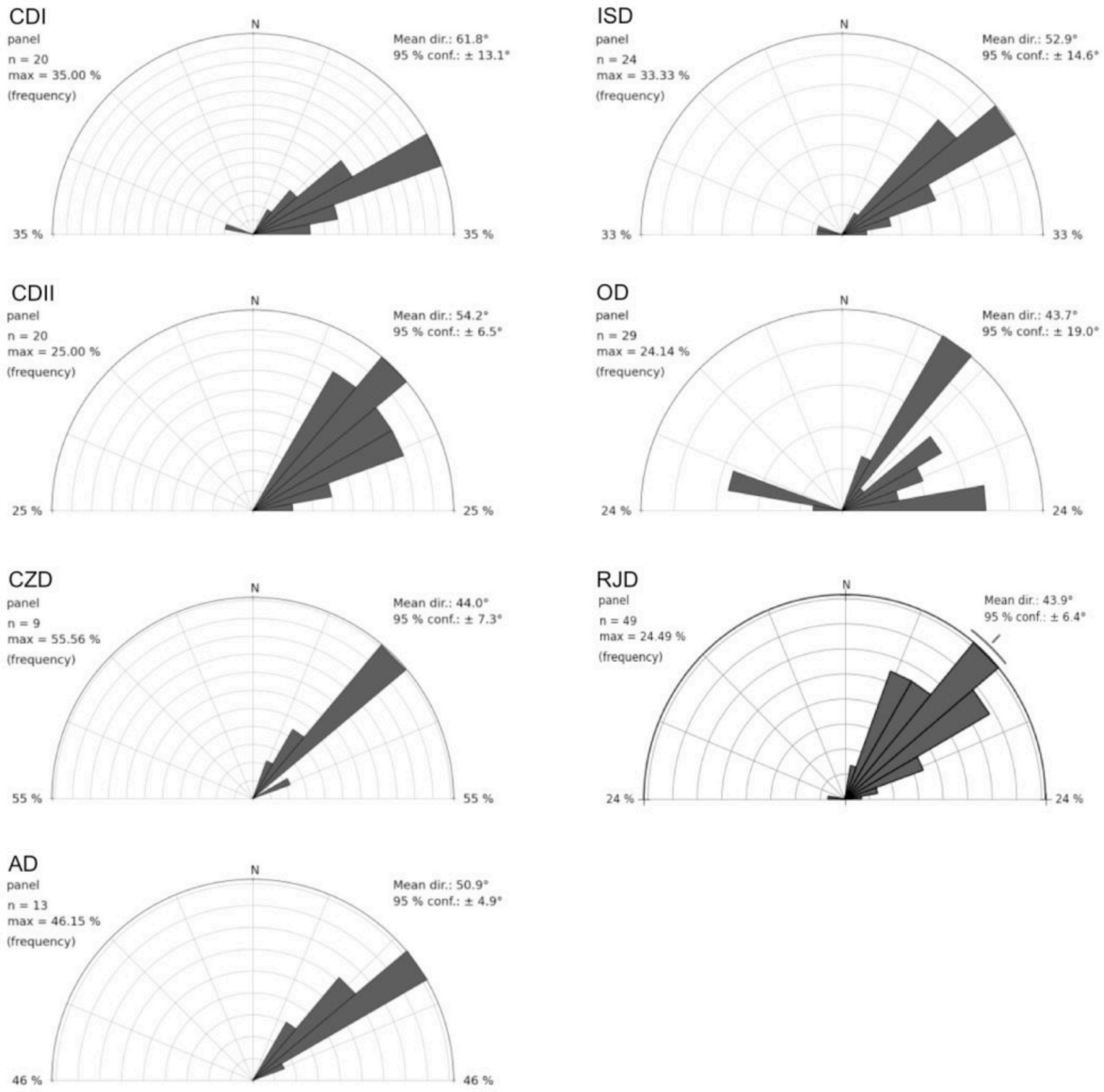

Fig. 6. Rose diagrams calculated for the orientation of the magnetic anomalies of each domain. CDI – Canindé Domain I; CDII – Canindé Domain Ii; CZD – Cruzeta Domain; AD – Arneiroz Domain; ISD – Intrusive Suites Domain; OD – Orós Domain; RJD – Rio Jucá Domain.

geometry. It considers that the gravity field is additive, i.e., the total field is the sum of the gravitational effects of the sources present in the region, from the surface to the upper mantle (Castro, 2005).

Density values were obtained from the literature (Blakely, 1996; Telford et al., 1990; Castro et al., 2002; Castro, 2011 and Pedrosa et al., 2015) and estimated through adjustment between the observed and the calculated curves, whereas the depth values were estimated from the solutions provided by analytical signal amplitude, curvature, and Euler deconvolution.

The 2D geological modelling was focused on determining the configuration of the shallower crustal levels that were estimated from previous regional studies, emphasizing the Cococi rift heterogeneity, as well as major lithostratigraphic units in the border region between Parnaíba Basin and Cococi Basin. The initial models were created based on surface geology data (Cavalcante et al., 2003), the 3D curvature, 2D analytic signal, and Euler deconvolution.

5. Results

5.1. Magnetic data

The anomalous magnetic field (Fig. 5a) has anomaly values with amplitudes ranging from −363.5 nT to 165.8 nT. The smallest values (−363.5 nT to 9.0 nT) are located below the Senador Pompeu shear zone, comprising the Rio Grande do Norte Domain, which is composed predominantly by gneiss. On the other hand, the highest values (9.0 nT to 165.8 nT) are located above the Senador Pompeu shear zone, belonging to the Ceará Central Domain, which has dikes and a predominance of basic rocks. The high amplitudes that are present in the Parnaíba Basin portion are related to the underneath extension of the Ceará Central and Rio Grande do Norte Domains, as well as partially the Cococi Basin.

The set of maps developed from magnetic data (Fig. 5a–d) was used to extract magnetic lineaments and to differentiate seven magnetic domains, which are shown separately in the vertical derivative map (Fig. 5c). Domain delimitation was defined by recognizing areas with magnetic anomalies of similar dimensions and orientations, based in

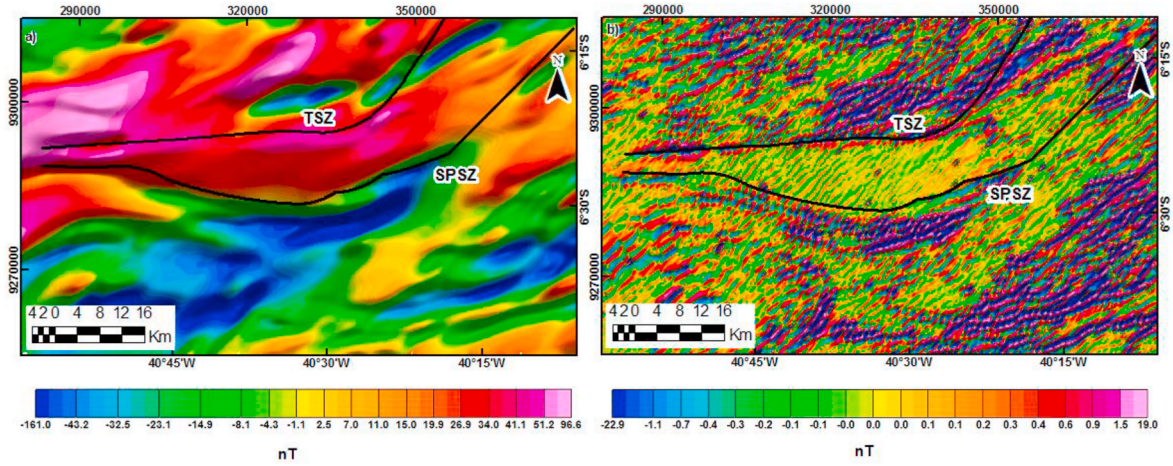

Fig. 7. Regional (a) and residual (b) magnetic maps derived from power spectrum analysis (Fig. 3). TSZ - Tauá shear zone, SPSZ - Senador Pompeu shear zone.

direction lineament show tilt derivative (Fig. 5d) and minima curvature (Fig. 9c). Futhermore, rose diagrams have been produced for domain comparison and to analyze each domain individually (Fig. 6). Generally, there is a preferential NE orientation all domains, but some E-W and WNW trends become evident in the southernmost Orós domain. These are attributed to the effects of the Orós-Jaguaribe sigmoidal shear zone. The seven domains with their outstanding characteristics are listed below. The magnetic lineament A', displayed in Fig. 5c, is oriented in NE direction, is coincident with barite occurrences and was referred to Cococi lineament by CPRM (1979).

The magnetic lineaments extracted from the map of the tilt signal inclination (Fig. 5d) show persistent longitudinal extensions and trends that average a NE direction. The shear zones, which controlled the opening of the Cococi Basin, become evident in certain locations, especially at the limits of the Basin, where various late reactivations associated with volcanic breccia and pyroclastic rocks were observed. Intrabasinal anomalies evidence small amplitudes and become enhanced in the vertical derivative and tilt derivative maps (Fig. 5c and d), showing consistent NE orientation with other lineaments. These features could be associated with the reactivation kinematics of the major regional shear zones.

The Cococi Lineament was defined by CPRM (1979) as the limit of between two grabens within the Cococi Basin, which were differentiated based on the characteristics of the sedimentary rocks. These included, fracture direction analysis, maturity, and post-sedimentation tectonic structures. The difference between the directions of the fractures is subtle since the eastern graben of the Cococi lineament presents predominant N37°W direction, and the western graben presents N50°W direction. CPRM (1979) highlighted that the constituent sediments of the eastern graben are less immature when compared to the western graben, their sedimentary layers are less disturbed in their compartments, and the fractures are longer in the longitudinal direction often showing signs of shear movement in greater evidence than in the western graben.

The regional magnetic anomalies display long-wavelength (>2.5 km), ranging from −96.6 nT to 27 nT, from west to east (Fig. 7a). This continuous increase of the magnetic anomaly can be explained by the intrusion of the Parnaíba Basin in Ceará Central Domain, influencing the framework of the Cococi Basin. The residual magnetic anomaly map (Fig. 7b) is represented by medium to long-wavelength (>2.5 km) negative and positive anomalies, the difference of anomaly, ranging from −22.9 nT to 19 nT, is in the amplitude of the magnetic signal, while the direction is predominantly NE-SW.

5.2. Magnetic domains

1 - Canindé Domain I: Situated to the northwest of the Basin and elongated in ENE direction, it shows anomalies with a mean amplitude of 60.47 nT. The preferential orientation of magnetic lineaments is N62°E, and dominant lithologies are metaplutonic and metasedimetary rocks of the Canindé Unit of the Ceará Group.

2 - Canindé Domain II: Located in the north part of the area, this domain has magnetic amplitudes that reach 124.20 nT within the anomalous field (Fig. 5a), suggesting the presence of a swarm of volcanic dikes intruded in the Neoproterozoic metamorphic Canindé Unit. Source depths range between 300 and 500 m depth estimates based on minimal curvature (Fig. 9a) and the magnetic lineaments have a mean N54°E trend, showing some smooth inflections due to the presence of the regional shear zones.

3 - Cruzeta Domain: Occupying the northeastern portion of the area, this domain extends in NE direction and has moderate amplitude values, with a maximum of 72.38 nT (Fig. 5a). These values may respond to intense tectonic-metamorphic migmatization and reworking processes that occurred in this zone, which may have produced a magnetic homogenization of the rocks. Magnetic lineaments are oriented towards the N44°E.

4 - Arneiroz Domain: Constitutes an area located to the south of the CB, which includes a belt of very low amplitudes with a mean calculated value of −10.07 nT (Fig. 5a), probably related to the high volume of quartzites present in the zone. The preferential orientation of magnetic lineaments is N51°E, with shallow depths ranging from 300 to depth estimates based on minimal curvature (Fig. 9a). However, in the sector occupied by the Parnaíba Basin, there is an overlap in the Arneiroz domain, which is more depth.

5- Intrusive Suites Domain: This southeastern domain holds the larger anomalies with a maximum of 149 nT corresponding to the syenogranitic to granitic Neoproterozoic intrusive suites. The magmatic lineaments strike N53°E.

6 - Orós Domain: Covering the southern portion of the area, this domain shows low magnetism in general, with a mean value of −18 nT. Lineament orientation prevalence is N44°E; nevertheless, significant divergences to E-W and NW-SE could be noticed and are attributed to the sigmoidal behavior of the Orós Group megastructure (Santos Filho et al., 2015). Similarly to the Arneiroz Domain, it corresponds to the sector that is covered by sedimentary rocks of the Serra Grande Group of the Paranaiba Basin

7 - Rio Jucá Domain: Located at the Cococi Basin, this domain shows a smooth texture in the magnetic maps reflecting anomalies of short amplitude with a mean value of −2.92 nT; this presents shallow sources because it is nearby Parnaiba Basin. The lineaments follow

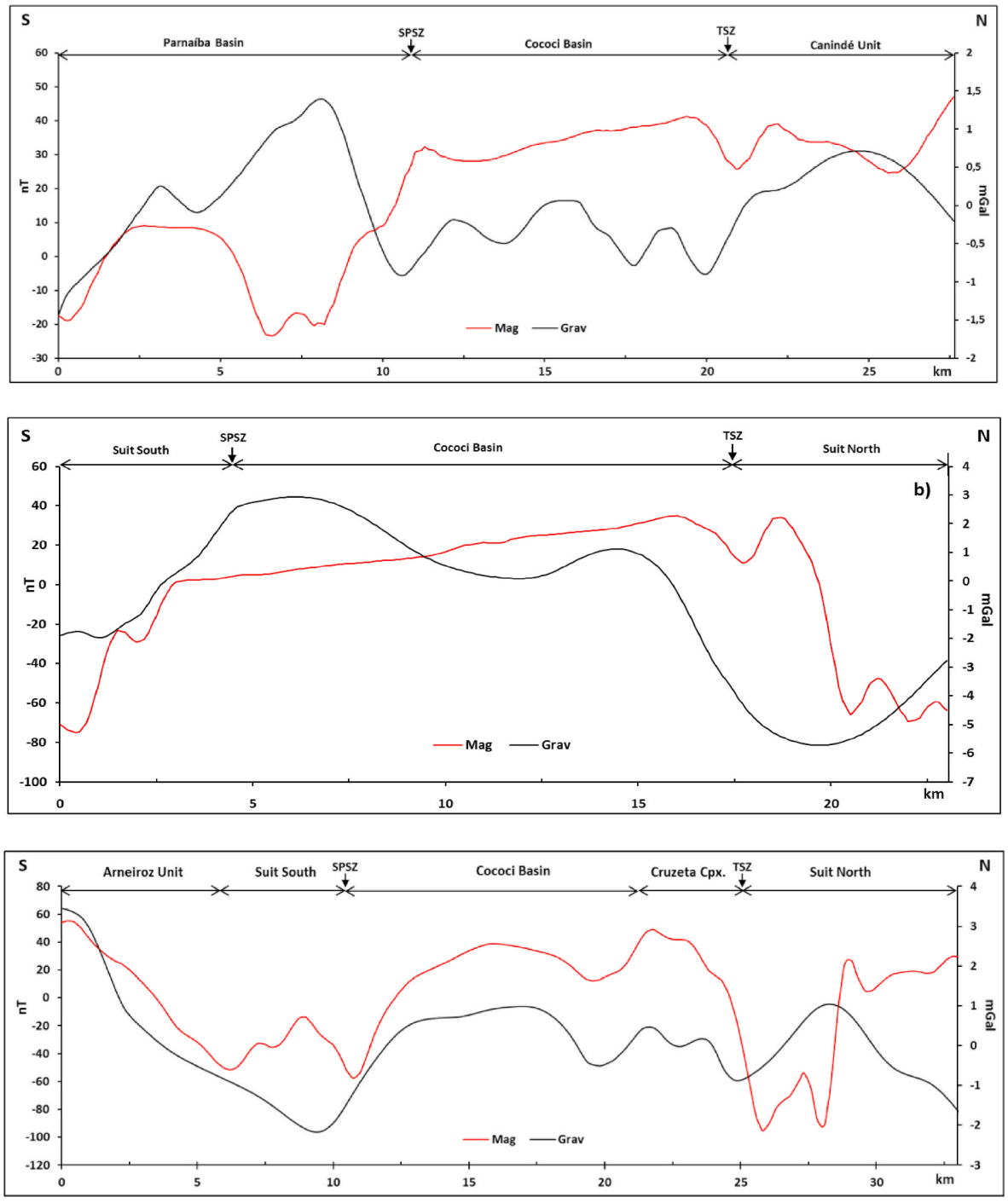

Fig. 8. Anomaly magnetic field (AMF) and gravimetric curves calculated for Secion (S1) (a), Secion (S2) (b) and Secion (S3) (c). See location of the sections in Fig. 4.

the regional trend (N44°E) and are related to fractures affecting the basement and the sedimentary rocks of the Jucá Group. The lineaments identified within the Cococi Basin were originated during its formation in response to the reactivation of the regional shear zones. Moreover, some reactivations that correlate Parnaiba Basin events were recognized (Godoy, 2010), with some of them hosting Fe-Cu mineralization and barite occurrences (Santos Filho et al., 2015).

5.3. Gravimetry

The limits between lithologies are evidenced by their density contrasts, facilitating the correlation of gravimetric and magnetic anomalies magnetic. Lithological boundaries correlated with gravimetric anomalies are used in all profiles, mainly the rift boundaries, which are evidenced by the gravimetric lows corresponding to Senador Pompeu and Tauá shear zones.

Anomalies within the Cococi Basin have small amplitudes as they are related to low-density rocks, and 2D modeling confirms that the Basin has a semi-graben structure. In section S1 (Fig. 8a), the limits of the Cococi Basin are well defined, whereas the Parnaiba Basin influence can be noted to the south, where the gravimetric effects of elevated basement portions tend to elevate the gravimetric values. Section S2 (Fig. 8b) crosscuts the Cococi Basin, including the Cococi lineament. Nevertheless, this structure does not show any magnetic or gravimetric anomaly

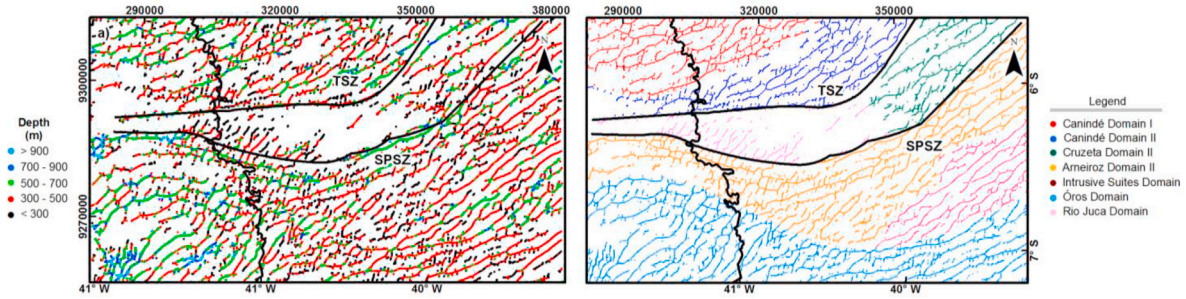

Fig. 9. a) Curvature solutions with depth estimates for lineaments and contacts; b) Extracted magnetic lineaments separated in seven domains according to their directions. TSZ – Tauá shear zone and SPSZ – Senador Pompeu shear zone.

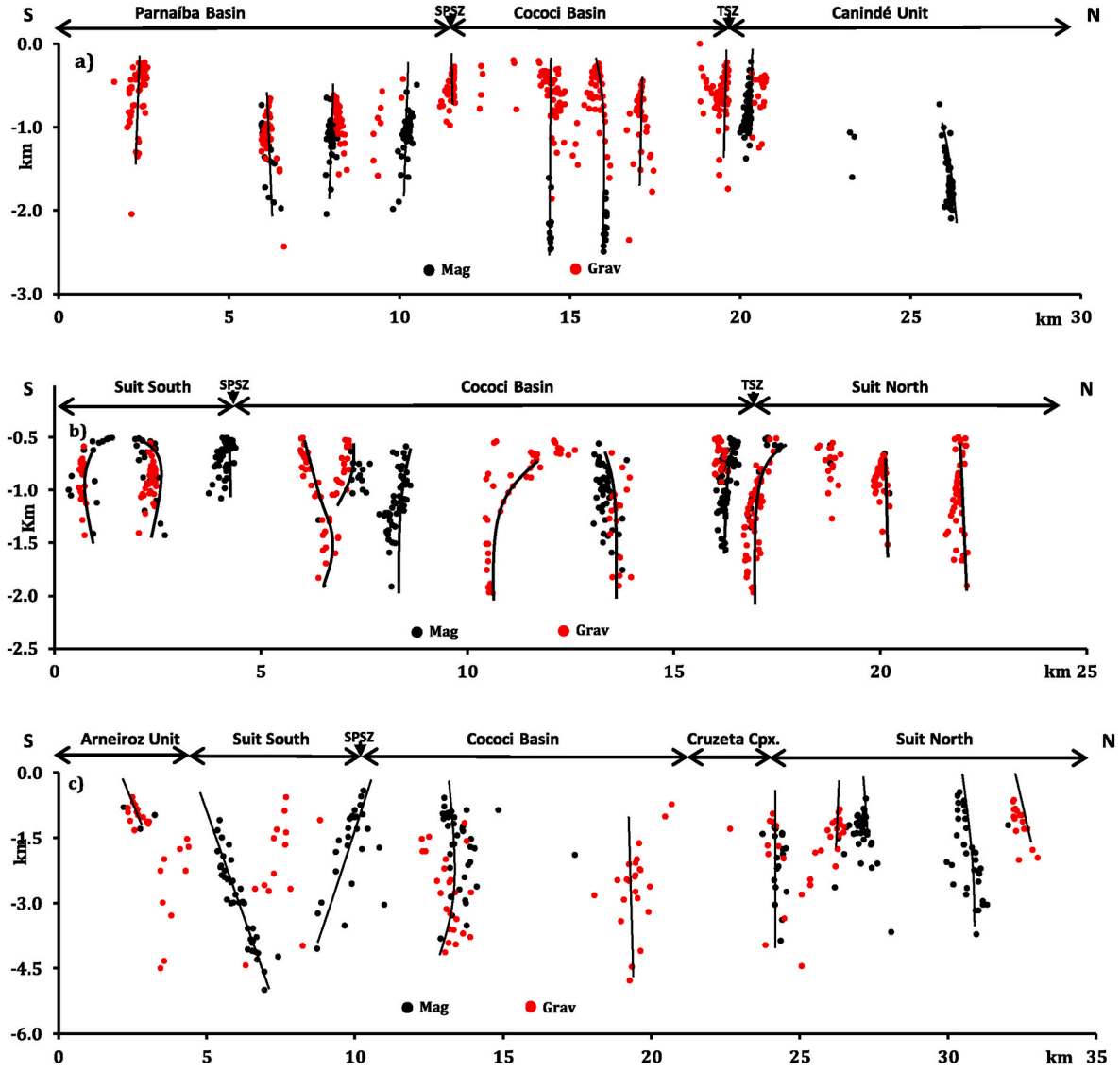

Fig. 10. Solution clouds obtained for 2D analytic signal amplitude processing. Sections S1 (a), S2 (b) and S3 (c) are represented. See location of the sections in Fig. 4.

that may be associated with the existing barite deposits. Differently from the other cases, in section S3 (Fig. 8c), the gravimetric and magnetic profiles have similar behaviors due to a relative increment in the magnetic values; this variation is probably associated with the proximity of the Basin's border.

5.4. Curvature

The obtained solutions were useful to identify magnetic domains, which were differentiated based on depth and direction criteria. As seen in Fig. 9, the depths found a range between 300 m and 500 m, with a few values overpassing 1000 m. The mean trend of the magnetic lineaments is N45°E, with some cases within the Orós-Jaguaribe domain showing

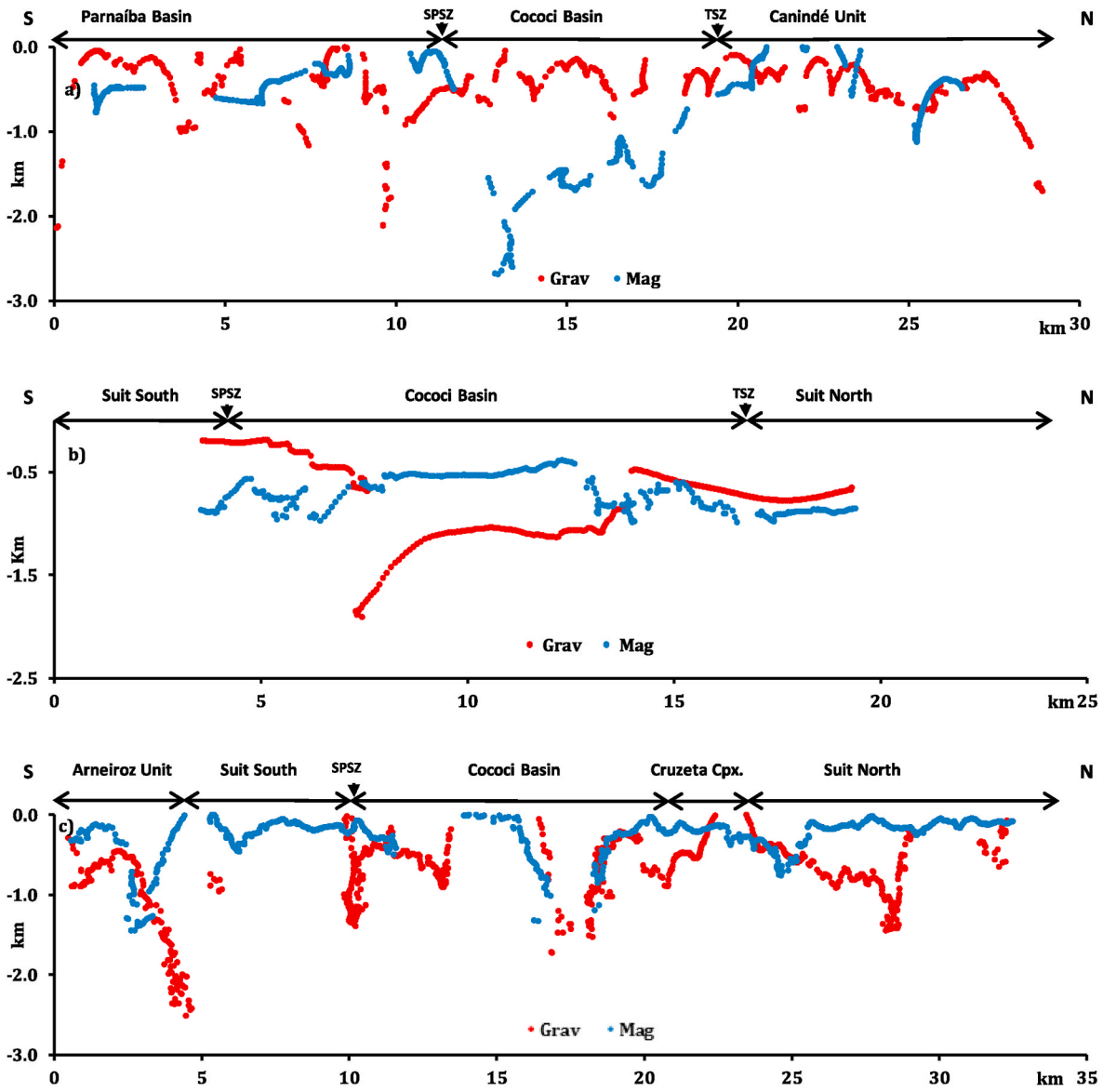

Fig. 11. Euler deconvolution solution for sections S1 (a), S2 (b) and S3 (c). See location of the sections in Fig. 4.

variations to the N20°W direction.

For the main faults, at the edge of the Cococi Basin, depths estimates were variable, from less than 700 m to more than 1000 m. In some cases, lineaments extend under the Parnaiba Basin, where they show greater depths than in the uncovered sectors.

5.5. Analytic signal amplitude

According to Castro et al. (2014), the main purpose of this method is to enhance depth in approximately vertical two-dimensional structures, such as dikes, fracture zones and faults. In this study, the solution clouds of magnetic and gravimetric data presented similar behavior, showing coincident inclinations and depths (Fig. 10a–c). In general, greater depths are observed within the Cococi Basin but fracture density increases outside the Basin.

Section S1 (Fig. 10a) shows deep faults within Parnaiba and Cococi Basins, with depths of about 1,9 and 2,7 km, respectively, both of them contrasting with Senador and Taua shear zones. The scarcity of structures in Canindé Unit is attributed to the low contrast between the anomalies corresponding to this lithology.

The concentration of deeper fractures at the Cococi Basin is also highlighted on section S2 (Fig. 10b) with depths over 1,5 km. The data clouds associated with ~1,5 km deep faults, located at the southern limit corroborate field observations and previous studies developed by Meneses (2012). Even though in this section, the Tauá shear zone reaches almost 2 km, the Senador Pompeu shear zone still appears to be shallow. It is noticeable that within this profile, several fractures exhibit inflections at low depths.

The solutions observed in section S3 (Fig. 10c) reveal outstanding increasing depths (up to 4,5 km) in the Senador Pompeu shear zone, as well as in the Cococi Basin faults, although the latter are reduced in number. Similar profound structures also define the contacts between the southern and northern intrusive suites with their host rocks (Arneiroz unit and Cruzeta Complex, respectively).

5.6. Euler deconvolution

According to Barbosa and Silva (2005), this method is used to obtain rapid interpretations of magnetic and gravimetric data attempting to eliminate the classical magnetic ambiguity caused by simultaneous estimate of magnetization intensity and the volume of the bodies, in order to estimate the depth of the sources. The gravimetric and magnetic

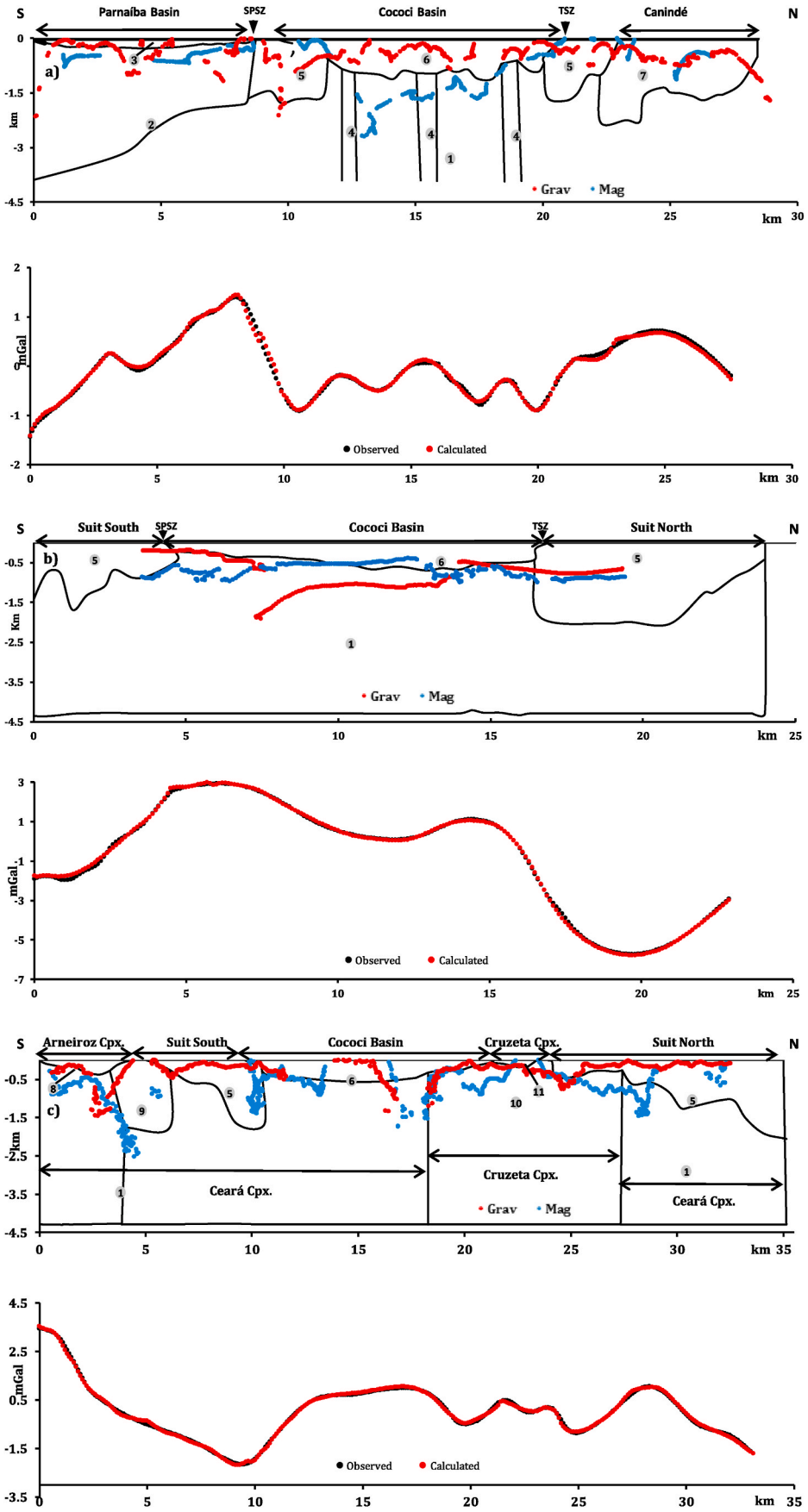

Fig. 12. 2D gravimetric modes for sections S1 (a), S2 (b) and S3 (c) showing the contouring of blocks with different densities. Euler deconvolution solutions are also included to facilitate comparison. For each section, a second diagram presents the observed and calculated curves. See the location of the sections in Fig. 4.

Table 1
Density values attributed to the different sources considered for 2D gravimetric modeling.

Crustal domain	Index	Geological unit	Lithology	Density (kg/m^3)
Ceará Central Domain	11	Cruzeta complex	Volcanic and cataclastic	2.68
	10		Gneisses and migmatites	2.72
	9	Intrusive suites	Granitoids	2.76
	8	Canindé unit	Meta sediments	2.70
	7	Arneiroz unit	Quartzite and schist	2.70
Cococi Basin	6	Rio Jucá group	Low grade metamorphic	2.54
	5	Intrusive suites	Granites	2.65
	4	Volcanic dikes	Basic to acid	2.90
Parnaíba Basin	3	Serra Grande group	Sandstones	2.50
	2	Basement	Gneisses	2.75
Upper crust	1	Basement	Volcanic	2.80

solutions obtained for each section are presented in Fig. 10.

Gravimetric solutions viewed in Section 1 (Fig. 11a) occur at depths varying from 50 to 2000 m, where the deeper points are probably associated with the contact between the Basin and the southern intrusive suite. In Section 2 (Fig. 11b), the gravimetric data suggest an asymmetric rift Basin with its main fault dipping southward and an antithetic fan beginning near the Senador Pompeu shear zone. Faulted blocks lay at estimated in depth between 200 and 500 m. Magnetic data define a horizontal surface that probably represents the basement of the Cococi Basin, while gravimetric data represent the limits of Cococi Basin. In Section 3 (Fig. 11c), Euler deconvolution solutions show well-defined line patterns with variable depths that could be interpreted as contact surfaces that delimitate the intrusive suites, the Cruzeta complex, and the Precambrian basement. Also, it is noticeable that within the Cococi Basin, the barite bearing Cococi lineament is enhanced by both solutions.

5.7. 2D gravimetric modeling

The results of Euler deconvolution, which aided with describing the geometry and thickness of the sedimentary package together with the analytic signal amplitude solutions that helped with defining contacts and fractures, gave support to develop 2D gravimetric models in vertical sections (Fig. 12). Previous studies such as Oliveira et al. (1972), Gomes et al. (2000), and Meneses (2012) were used to determine constraints for the models. According to these authors, the CB is formed by two half-grabens, controlled by normal faults, and composed by different lithologies. In this work, the NE-SW striking faults, that control the Basin's structure within the studied area were inferred by combining the analytic signal amplitude and minimum curvature methods. For generating the initial model, it was considered eleven gravimetric sources of significant expression. The density values adopted for each source were either estimated through the adjustment between the observed and the calculated curves or obtained from previous work that dealt with equivalent lithologies (Table 1). For the main basement, which was assumed to be composed of gneisses, granitic intrusions, and sporadic basaltic dikes, a mean density value of 2.8 kg/m^3 was used in agreement with similar studies carried out in nearby areas (Cavalcante, 1999; Osako et al., 2011). Within the area of section S1, bimodal volcanism, mainly expressed by volcaniclastic lithologies, has been recognized in the Cococi Basin, and a density value of 2.8 kg/m^3, has been determined for these units. Considering that granitic rocks are rich in K-feldspar and plagioclase (Arthaud, 2007), their estimated density value was 2.65 kg/m^3. For the Parnaiba sedimentary basin unit that appears in the study area, Jaícos Formation and the Basin's basement rocks (gneisses, amphibolites, and granitoids), it was adopted the density values of 2.45 kg/m^3 and 2.75 kg/m^3, respectively, which were determined by Castro (2011). The granitic intrusions which constitute the basement of the Cococi Basin in sections 1 and 2 have been intensely fractured and intruded by mantle-derived material, following a density of 2.65 kg/m^3 was adopted for this association (value also corroborated by the adjustment between curves). The density of 2.55 kg/m^3 estimated for the sedimentary sequence of the Cococi rift is coincident with the value used by Castro (2011), and the estimated thickness of the sequence was of 1 km in section S1. For the Ceará complex, Osako et al. (2011) and Pedrosa Jr et al. (2015) reported density values of 2.68 kg/m^3 and 2.72 kg/m^3, respectively, which agree with the calculated value of 2.7 kg/m^3 for both the Canindé and Arneiroz units. For the Cruzeta complex, it was adopted the density value of 2.72 kg/m^3 that was used by Cavalcante (1999), whereas for the mylonitic rocks, which border this complex, it was estimated a value of 2.67 kg/m^3.

A tectonic influence of the Parnaíba Basin was inferred on section S1, probably associated with the bimodal volcanism recognized in the Cococi Basin, mainly expressed by volcaniclastic lithologies.

Section S2 (Fig. 12b) has an N-S orientation aiming to cut the NE-SW trending Cococi lineament (Fig. 5c), which, according to Oliveira et al. (1972), constitutes the limit between the two asymmetric half-grabens that within the Cococi Basin. This model has been developed with

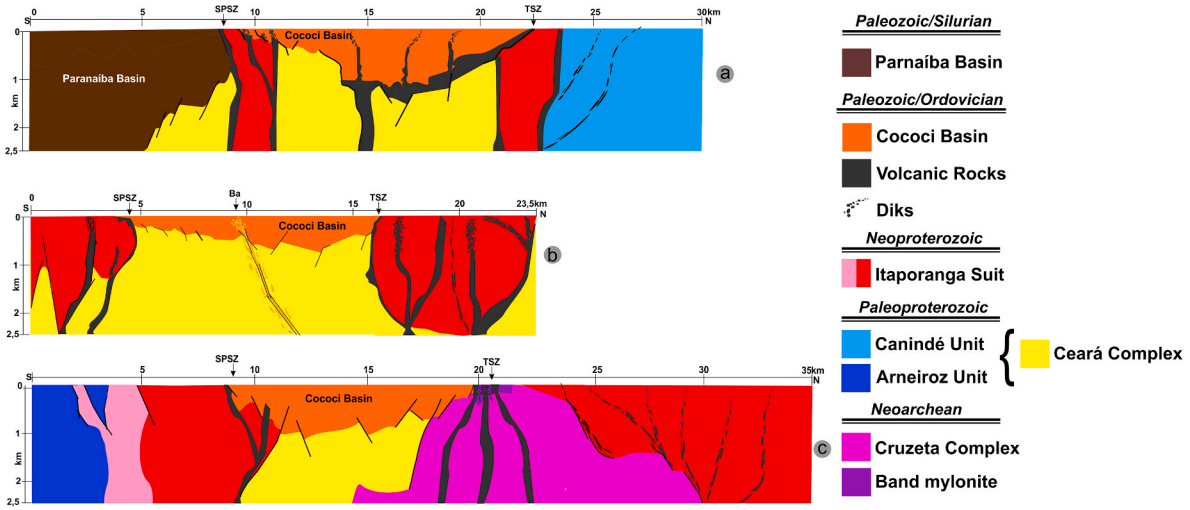

Fig. 13. Geological models for sections S1 (a), S2 (b) and S3 (c), generated after the integrated interpretation of the magnetometric and gravimetric processed results.

four gravimetric sources: the basement of rocks, the Basin's sedimentary package and the southern and northern intrusive suites. The geometry of the modeled Basin resembles a northward deepening half-graben with its axis oriented E-W, characteristics that could also be appreciated in the Euler deconvolution solutions (Fig. 11b). With an estimated depth of 650 m, the depocenter is situated in the north portion of the Basin. The Cococi lineament, which has been associated with basement fracturing and hydrothermal occurrences (Santos Filho et al., 2015), as well as the Basin's generating faults, have been highlighted in the model.

Section S3 (Fig. 12c) crosscuts all the Cococi Basin formations, Arneiroz and Canindé units, both intrusive suites, and the Cruzeta complex, showing the modeled contacts between these units. In this section, the Cococi Basin presents an inverted geometry (relative to section S2), showing a southward deepening half-graben with a maximum depth of 1 km at the southern portion of the rift.

The integrated interpretation of the results led to the development of three geological models corresponding to the three surveyed sections (Fig. 13a to c), where new geological features not acknowledged in previous studies are exposed.

6. Discussion and conclusion

The integrated interpretation of the results led to the development of three geological models corresponding to the three surveyed sections (Fig. 13a to c), where new geological features not acknowledged in previous studies are exposed.

Gravimetric and magnetometric modeling confirm shear and deep faults reaching 4 km or more. These lineaments are responsible for the Basin structure and subsequent reactivations of fracturing and failing the sediments and volcanic of the Basin. The volcanic rocks are found in the basement and in granites. On the limits of the Basin, there are metric dikes of basalts, which proves that faulting affects the Precambrian and has a connection with mantle magma.

The Cococi Basin is divided by the N-S Cococi lineament into two antithetic half-grabens with opposite vergencies. The western half-graben, represented by the geological model presented in section S2 (Fig. 13b), deepens northward and has an E-W oriented axis with a maximum depth of 1000 m. A strong post-rift influence of the Parnaíba Basin is considered to affect the western portion of the Cococi Basin, suggested by the presence of faults reactivations structures on the Basins border. This reactivation occurred at the tectonic boundary between the granite and the basement, building the eastern boundary of Cococi Basin. Basaltic and rhyolite volcanism is the last volcanic activity within the Cococi Basin, as it cuts into other sedimentary lithologies and border granites. Barite deposits that occur at the limits between Basin's half-grabens are interpreted to be associated with fault-reactivations.

At Section S2 (Fig. 13b), this same half-graben is limited by the Cococi lineament and appears to be shallower, showing a depth of about 500 m. The eastern half-graben, modeled in section S3 (Fig. 13c), presents an inverted geometry, deepening southward and having its axis oriented ENE-WSW, with a maximum depth of 1 km at the southern portion of the rift. In this model, it is proposed that the basement of the Cococi Basin near the border is partially formed by Cruzeta Complex portions. In this section, the Basin presents asymmetry, with the northern part deeper than the southern part by at least 200 m of difference. In general, the Eopaleozoic Basins are associated with mantle plume ascendance that may lead to a rifting process forming volcaniclastic rocks. As illustrated in section S1 (Fig. 13a), within the Cococi Basin, the upwelling of mantle-derived material occurred mainly the northern and southern limits of the Basin through extensional fractures that generated the Miranda Formation dikes (500–452 My), appearing to be contemporaneous with the Cococi rift (Santos Filho et al., 2015). This fact is also documented by the presence of volcanoclastic rocks among the Basin's conglomerates.

Through overall analysis, it could be observed that the identified NE-SW magnetic lineaments follow the regional trend of the Central Ceará domain, in which the CB is inserted. The combined kinematics of the sinistral Tauá shear zone and dextral Senador Pompeu shear zone generated a trans-tensional regime in the terrain comprised between both shear zones. The fragile extensional deformation has litho-structural field expressions such as cataclastic rocks associated with volcanic lithologies and abundant sub-volcanic rocks intruding extensional fractures. In Section S2, it can be noted that the Cococi Basin is wider and less deep than in the other sections. The faults are predominantly listric and converge to the central part of the Basin.

The limits and depth of the Basin, some of its internal main structures, as well as the contacts between the associated lithological units, have been modeled with good resolution. As the obtained solutions are coherent with geological field observations, cartography, and previous works, it was concluded that potential methods have been used satisfactorily to investigate the structural features of the Cococi Basin and its basement.

Declaration of competing interest

The authors declare that they have no known competing financial interests or personal relationships that could have appeared to influence the work reported in this paper.

Acknowledgments

This work is part of the master dissertation of the first author, linked to the post-graduate program of the Federal University of Ceará, Brazil. The authors would like to thank the Brazilian Geological Survey (CPRM) for geophysical data yielding. The support of friend Nilton Cesar that always helped. The first author is also grateful to Coordenação de Aperfeiçoamento de Pessoal de Nível Superior (CAPES) for the research fellowship and to the Laboratório de Geofísica de Prospecção e Sensoriamento Remoto (LGPSR) of the Universidade Federal do Ceará (UFC) for allowing the use of the facilities for data processing and interpretation.

References

Arthaud, M.H., 2007. Evolução Neoproterozóica Do Grupo Ceará (Domínio Ceará Central NE Brasil): Da Sedimentação Às Colisão Continental Brasiliana. Tese de Doutorado. Ins. Geoc., UNB, Brasília, pp. 33–50.

Barbosa, V.C.F., Silva, J.B.C., 2005. Deconvolução de Euler: passado, presente e futuro - um tutorial. Rev. Bras. Geofísica, Rio de Janeiro/RJ 23 (3), 243–250.

Billings, S.D., Richards, D., 2000. Quality Control of Gridded Aeromagnetic Data. Geosoft, p. 68. http://www.geosoft.com.

Blakely, R.J., 1996. Potential Theory in Gravity and Magnetic Applications, second ed. Cambridge University Press, Cambridge (UK, p. 441.

Castro L, David, 2005. Modelagem gravimétrica 3-D de corpos graníticos e bacias sedimentares com embasamento estrutural de densidade variável. Revista Brasileira de Geofísica 23 (3), 295–308.

Castro, D.L., 2011. Gravity and magnetic joint modeling of the Potiguar Rift Basin (NE Brazil): basement control during Neocomian extension and deformation. J. S. Am. Earth Sci. 31, 186–198.

Castro, D.L., Branco, R.M.G.C., Martins, G., Castro, N.A., 2002. Radiometric, magnetic, and gravity study of the Quixadá Batholith, Central Ceará Domain (NE-Brazil): evidence for an extension controlled emplacement related to the Pan-African/ Brasiliano collage. J. S. Am. Earth Sci. 15 (5), 543–551.

Castro, D.L., Bezerra, F.H., Sousa, M.O., Fuck, R.A., 2012. Influence of Neoproterozoic tectonic fabric on the origin of the Potiguar Basin, northeastern Brazil and its links with West Africa based on gravity and magnetic data. J. Geodyn. 54, 29–42.

Castro, D.L., Fuck, R.A., Phillips, J.D., Vidotti, R.M., Bezerra, F.H.R., Dantas, E.L., 2014. Crustal structure beneath the Paleozoic Parnaíba Basin revealed by airborne gravity and magnetic data. Braz. Tectonophys. Amst. 614, 128–145.

Cavalcante, J.C., 1999. Limites e evolução do sistema Jaguaribeano, Província Borborema, Nordeste do Brasil. Universidade Federal do Rio Grande do Norte, Master's thesis, p. 169 (il).

Cavalcante, J.C., Vasconcelos, A.M., Medeiros, M.F., Paiva, I.P., Gomes, F.E.M., Cavalcante, S.N., Cavalcante, J.E., Melo, A.C.R., Duarte Neto, V.C., Benevides, H.C., 2003. Mapa geológico do Estado do Ceará, escala 1:500.000. Fortaleza, Ministério das Minas e Energia. Companhia de Pesquisa de Recursos Minerais.

Cordell, L., Grauch, V.J.S., 1985. Mapping basement magnetization zones from aeromagnetic data in the San Juan Basin, New Mexico. In: The Utility of Regional Gravity and Magnetic Anomaly Maps. Society of Exploration Geophysicists, pp. 181–197.

CPRM, DNPM, Convênio DNPM/CPRM, 1979. Projeto Borda Leste da Bacia do Maranhão (Levantamento aeromagnetométrico e aerogamespectrométrico), Relatório Final, Volumes I e II (Rio de Janeiro).

Doo, W.B., Hsu, S.K., Yeh, Y.C., 2007. A derivative-based interpretation approach to estimating source parameters of simple 2D magnetic sources from Euler deconvolution, the analytic-signal method and analytical expressions of the anomalies. Geophys. Prospect. 55, 255–264.

Fetter, A.H., Van Schmus, W.R., dos Santos, T.J.S., Neto, J.A.N., Arthaud, M.H., 2000. U-Pb and Sm-Nd geochronological constraints on the crustal evolution and basement architecture of Ceará state, NW Borborema province, NE Brazil: implications for the existence of the paleoproterozoic supercontinent" Atlantica. Rev. Bras. Geociencias 30 (1), 102–106.

GM-SYS, 2004. Gravity/Magnetic Modeling Software: User's Guide Version 4.9. NGA Inc., p 101

Godoy, D.F., 2010. Evolução Termocronológica pro Traços de Fissão em Apatita e Zircão das Bacias da Transição Proterozóico – Fanerozóico de Camaquã (RS), Castro (PR), Eleutério (SP/MG), Jaibaras e Cocoi (CE). Tese de Doutorado. UNESP. São Paulo 141.

Gomes, J.R.C., Vasconcelos, A.M., Torres, P.F.M., 2000. Programa de Levantamentos Geológicos Básicos do Brasil, Programa Jaguaribe SW, Folha SB.24-Y, escala 1: 500.000. Fortaleza, de Pesquisa de Recursos Minerais, p. 167.

Hood J, Peter, Teskey J, Dennis, 1989. Aeromagnetic gradiometer program of the Geological Survey of Canada. Geophysics 54, 1012–1022.

Keating, P.B., 1998. Weighted Euler deconvolution of gravity data. Geophysics 63, 1595–1603.

Macleod, I.N., Vierra, S., Chaves, A.C., 1993a. Analytic signal and reduction-to-the-pole inthe interpretation of total magnetic field dataat low magnetic latitudes. In: Proceedings of the Third International Congress of the Braziliansociety of Geophysicists.

MacLeod, I.N., Jones, K., Dai, T.F., 1993b. 3-D analytic signal in the interpretation of total magnetic field data at low magnetic latitudes. Explor. Geophys. 24 (4), 679–688.

Martins, G., Oliveira, E.P., Lafon, J.M., 2009. The Algodões amphibolite-tonalite gneiss sequence, Borborema Province, NE Brazil: geochemical and geochronological evidence for Paleoproterozoic accretion of oceanic plateau/back-arc basalts and adakitic plutons. Gondwana Res. 15, 71–85.

Meneses, L.B., 2012. Mapeamento Geológico e Aspectos Tipológicos das Ocorrências de Cobre da Porção Oeste da Bacia Eo-Paleozoica do Cococi-Ce. In: Relatório de Graduação. Dep. Geologia, UFC. Fortaleza, Ce, p. 101.

Miller G, Hugn, Sing, Vijay, 1994. Potential field tilt—a new concept for location of potential field sources. Journal of Applied Geophysics 32, 213–217.

Nabighian, M.N., 1972. The analytic signal of two-dimensional magnetic bodies with polygonal cross-section: its properties and use for automated anomaly interpretation. Geophysics 37 (3), 507–517.

Nabighian, M.N., 1974. Additional comments on the analytic signal of two-dimensional magnetic bodies with polygonal cross-section. Geophysics 39 (1), 85–92.

Oliveira, K.M.L., de Castro, D.L., Branco, R.M.G.C., de Oliveira, D.C., Alvite, E.N., Jucá, C.C., Branco, J.L.C., 2018. Architectural framework of the NW border of the onshore Potiguar Basin (NE Brazil): an aeromagnetic and gravity based approach. J. S. Am. Earth Sci. 88, 700–714.

Oliveira C, João, Ferreira A, Cícero, Forte P, Fernando, Barros L, Francisco, Convênio DNPM/CPRM, 1972. Projeto Cococi. http://rigeo.cprm.gov.br/jspui/handle/doc/2736.

Osako, L.S., Castro, D.L., Fuck, R.A., Castro, N.A., Pitombeira, J.P.A., 2011. Contribuição de uma Seção Gravimétrica Transversal ao Estudo da Estruturação Litosférica na Porção Setentrional da Província Borborema, NE do Brasil. Rev. Brasileira Brasileira de Geofísica. 29 (2), 309–329.

Parente, C.V., Arthaud, M.H., 1995. O sistema Óros-Jaguaribe no Ceará, NE do Brasil. Rev. Bras. Geociencias 25 (24), 297–306.

Parente, C.V., Filho, W.F.S., Almeida, A.R., 2004. Bacias do Estágio de Transição do Domínio Setentrional da Província Borborema (Parte Integrante do Texto Bacias Do Estágio Da Transição Da Plataforma Sul-Americana. In: Neto, V.M., Bartorelli, A., Carneiro, C.D.R., Neves, Brito, B B (Eds.), Desvendar de um Continente: A Moderna Geologia da América do Sul e o Legado da Obra de Fernando Flávio Marques de Almeida, vol. 1, pp. 525–536. Org.

Pedrosa Jr., N.C., Vidotti, R.M., Fuck, R.A., Oliveira, K.M.L., Branco, R.M.G.C., 2015. Structural framework of the Jaibaras Rift, Brazil, based on geophysical data. J. S. Am. Earth Sci. 58, 318–334.

Phillips, J.D., Hansen, R.O., Blakely, R.J., 2007. The use of curvature in potential-field interpretation. Explor. Geophys. 38 (2), 111–119.

Roest, W.E., Verhoef, J., Pilkington, M., 1992. Magnetic interpretation using 3-D analytic signal. Geophysics 57, 116–125.

Santos Filho, F.F.B.D., Magini, C., Branco, R.M.G.C., 2015. Interpretação das assinaturas geofísicas relacionadas a estrutura da Bacia de Cococi e mineralizações de barita-SW do CE. Rev. Geol. 28 (2), 79–100.

Soares, R.D., 2011. Modelagem 2D de dados gravimétricos do Rifte Guaritas como contribuição ao conhecimento da evolução tectônica da Bacia do Camaquã. Dissertação de Mestrado. Dep. Geologia, UFRGS, Porto Alegre, RS, p. 114.

Talwani, M., Heirtzler, J.R., 1964. Computation of magnetic anomalies caused by two dimensional bodies of arbitrary shape. In: Parks, G.A. (Ed.), Computers in the Mineral Industries, Part 1, vol. 9. Stanford University Publications, Geological Sciences, pp. 464–480.

Talwani, M., Worel, J.L., Landisman, M., 1959. Rapid gravity computations for two dimensional bodies with application to the Mendocino submarine fracture zone. J. Geophys. Res. 64, 49–59.

Telford, W.M., Geldart, L.P., Sheriff, R.E., 1990. Applied Geophysics. Cambridge university press.

Vasconcelos, A.M., Gomes, F.E.M., 1998. Programa Levantamentos Geológicos Básicos Do Brasil-Iguatu (Folha SB. 24-Y-B) 1: 250.000. Fortaleza. CPRM.

Won, I.J., Bevis, Michael, 1987. Computing the gravitational and magnetic anomalies due to a polygon: algorithms and Fortran subroutines. Geophysics 52 (2), 232–238.